EARTH SURFACE PROCESSES AND LANDFORMS, VOL. 21, 195–203 (1996)

SHORT COMMUNICATION

USING SPECTRAL ANALYSIS TO DETECT SENSOR NOISE AND CORRECT TURBULENCE INTENSITY AND SHEAR STRESS ESTIMATES FROM EMCM FLOW RECORDS

M. F. LAPOINTE

Geography Department, McGill University, Canada

B. DE SERRES, P. BIRON AND A. G. ROY

Département de géographie, Université de Montréal, Canada

Received 6 June 1994
Accepted 16 May 1995

ABSTRACT

Electromagnetic current meters (EMCMs) are frequently used to gather turbulent velocity records in rivers and estuaries. Experience has shown that, on occasion, the output of these sensors can be affected by contamination from various noise sources. These noises may be limited to narrow bands of frequencies and thus fail to produce conspicuous increases in observed signal variance. Such 'narrow-band' noises can be difficult to identify from simple inspection of signal traces or variance levels, yet degrade estimates of turbulence statistics, in particular covariances (used to calculate Reynolds shear stress). This paper demonstrates the usefulness of spectral analysis to detect and characterize narrow-band noise components in turbulent flow records. Statistical principles underlying the use of spectral analysis for noise detection are briefly reviewed. Examples of u and v velocity spectra and cospectra are then presented from actual EMCM velocity records from flume and field deployments that were found to be contaminated by such noises. The sensitivity of the shear stress estimates to even minor noise levels is demonstrated. The use of spectral analysis to correct variance (turbulence intensity) and covariance (shear stress) estimates obtained from records contaminated by narrow-band noise is also illustrated.

KEY WORDS spectral analysis; turbulence; electromagnetic current meters; noise; river hydraulics

INTRODUCTION

In many field studies of turbulent alluvial flows, time records of fluctuating horizontal ($u(t)$) and vertical ($v(t)$) velocities are collected using electromagnetic current meters (EMCMs) deployed at various points over an alluvial boundary (e.g. Clifford *et al.*, 1993). Physical parameters such as turbulence intensity and eddy mixing coefficients can be estimated from the observed variances of the flow components. Reynolds shear stresses are also important parameters of turbulent shear flows, estimated from the covariance of the measured u, v and w (lateral) flow components (Heathershaw, 1979; Williams *et al.*, 1989). In particular, the streamwise Reynolds shear stress (both mean, $-\rho\overline{uv}$, and instantaneous, $-\rho u'v'$) has been shown to be a fundamental parameter in sediment-transport studies.

EMCMs are relatively inexpensive and physically robust flow sensors. The linearity and directional response of different EMCM models in steady and oscillating flows have been investigated by several researchers (Aubrey and Trowbridge, 1985; Guza *et al.*, 1988; Lane *et al.*, 1993). Their bidirectionality and moderately high frequency response has made them extremely useful instruments for turbulence work in rivers. However, EMCM design relies on major amplification of minute voltages induced by the flow surrounding the probe, a process that can render these sensors somewhat noisy. Although such problems are usually de-emphasized in research publications, EMCM output has quite often been observed

CCC 0197–9337/96/020195–09

to be contaminated by a range of noise sources (McQuivey, 1973; Lapointe, 1990; Lane *et al.*, 1993), whether because of intermittent contact of suspended debris with the sensor electrodes, the presence of ambient electromagnetic fields or undue motion of the sensor cable. Extraneous noises may degrade variance and covariance estimates from turbulent flow records. Undetected noises also have the potential to severely mar any 'event-based' study of the time records, such as the quadrant analysis introduced by Willmarth and Lu (1972). The growing use of EMCM sensors in wide-ranging environments requires that new users be skilled at dealing with occasional noise problems, an issue that has received relatively scant attention in the literature.

In many instances, external noises can be readily identified from inspection of velocity traces or from the statistics of the velocity signals. This paper will illustrate more problematic cases where subtle contamination, affecting only a narrow band of frequencies, may not be detected through such simple tests and yet may significantly affect signal statistics. Spectral techniques will be used to identify such 'narrow-band' contamination in these records. A theoretical section will first summarize basic statistical principles underlying the use of spectral analysis in this context. These principles are then applied to two examples of EMCM signals obtained from actual field and flume deployments affected by such noise effects. The focus of the paper is on the simple case of random noise fluctuations that are statistically independent of the true flow signal, although more complex noise problems can of course occur. It is also assumed in what follows that, through previous studies of the given class of flow, the general shape of the turbulent spectra are known and that the records under study are long enough to be analysed spectrally with reasonable precision.

The analysis will emphasize the spectral characteristics of actual corrupted signals, as well as the possibility for correction of variance and covariance estimates derived from the records. The basic principles of noise detection discussed below are general and may be used with turbulence data from sensors other than EMCMs or, with appropriate modifications, to more complex noise models. Neither the problem of the physical origin of EMCM noises, nor the effects of extraneous noises on quadrant analysis of turbulent 'events' can be discussed in this short paper. However, detecting the presence of extraneous noises is a first requirement to address these problems, and the analytical techniques discussed below are useful to this end.

THEORY

An 'observed' flow velocity signal sampled at the sensor output $u_0(t)$ can be expressed as the sum of a true flow component signal $u(t)$ and of a noise term $n(t)$:

$$u_0(t) = u(t) + n(t) \tag{1}$$

Note that the noise term $n(t)$ is not a constant but rather is itself a fluctuating, random signal resulting from disturbances to output other than those driven by flow around the sensor. These disturbances may be generated internally in the sensor (e.g. amplifier noise) or from the overall sensor environment (e.g. noises due to external electromagnetic (EM) fields). In the general case, n and u fluctuations may be correlated. From Equation 1 it follows that the variance of the observed signal is given by

$$\sigma^2_{u_0} = \sigma^2_{u+n} = \sigma^2_u + \sigma^2_n + 2\sigma^2_{un} \tag{2}$$

where σ^2 is the variance and σ^2_{un} is the covariance between u and n. The following general identity determines the size of this covariance:

$$\sigma^2_{un} = \sqrt{\sigma^2_u \sigma^2_n}\, r_{un} \tag{3}$$

where r_{un} is the correlation coefficient between u and n fluctuations.

In the cases where the noise and flow signals $n(t)$, $u(t)$ are driven by statistically independent (thus uncorrelated) processes, r_{un} is zero and from Equations 2 and 3 (Bendat and Piersol, 1986):

$$\sigma^2_{u_0} = \sigma^2_u + \sigma^2_n \tag{4}$$

The presence of such a noise component thus always increases the observed velocity variance.

Noise components may of course be multiplicative rather than additive, or partially correlated with the

true flow signal. Nonetheless, additive and independent noise models are often realistic and useful (Bendat and Piersol, 1986). Stray fluctuations in sensor output, driven, for example, by extraneous EM fields, may not be appreciably correlated with the true signal, i.e. the flow fluctuations within a small sensing volume surrounding the instrument. It will be seen later that the simple assumption of noise independence produces a reasonable description of cases of EMCM noises analysed in this paper.

A common procedure to identify and eliminate from further analysis very noisy segments embedded within long records is to plot variances for successive time segments. By Equation 4, assuming the true flow signal to be stationary, strongly contaminated segments on average show higher variances. However, this data editing procedure may fail to identify some noise effects, given the inherent variability in segment-to-segment sample variances as well as the possibility that the noise may be present over the length of the velocity record. In particular, moderate intensity, narrow-band noises may contribute weakly to the overall variance of u, which integrates variance contributions over all frequencies. It will be shown next that even minor noises can appreciably mar covariance estimates.

Covariance contamination by noises

The effects on the uv covariance (and shear stress estimates) of relatively minor levels of noise can be worrisome where a common noise mechanism contaminates the two channels $\overline{u, v}$ simultaneously. When noises occur on EMCM output, they often affect both channels. Noises due to sudden sensor cable motion, sensor platform vibration or ambient EM fields created by power lines, electric motors or generators generally affect both channels. The particular sensitivity of covariance estimates to bi-channel noises can be illustrated by an idealized case where u and v signals are both affected by an identical noise component n (the time subscript of the flow and noise fluctuations is now omitted for simplicity):

$$u_0 = u + n;\ v_0 = v + n \tag{5}$$

The observed uv covariance is then given by:

$$\sigma^2_{u_0 v_0} = \sigma^2_{uv} + \sigma^2_{un} + \sigma^2_{vn} + \sigma^2_n \tag{6}$$

If the noise fluctuations over long records are essentially uncorrelated with u and v fluctuations, then Equation 6 simplifies to:

$$\sigma^2_{u_0 v_0} = \sigma^2_{uv} + \sigma^2_n \tag{7}$$

From Equation 7, the error on the observed uv covariance estimate equals the variance of the noise itself.

Such noises, in effect, produce a bigger relative error on the covariance than on the individual u, v variance estimates. Indeed, combining Equations 7 and 3, the fractional error (in absolute value) on the covariance estimate due to the noise can be estimated as:

$$\frac{\sigma^2_n}{|\sigma^2_{uv}|} = \sqrt{\frac{\sigma^2_n}{\sigma^2_u}\frac{\sigma^2_n}{\sigma^2_v}}\,\frac{1}{|r_{uv}|} \tag{8}$$

Assuming, for example, a typical value of $-0{\cdot}4$ for r_{uv} in boundary layers (McQuivey, 1973b), Equation 8 becomes:

$$\frac{\sigma^2_n}{|\sigma^2_{uv}|} = 2{\cdot}5\sqrt{\frac{\sigma^2_n}{\sigma^2_u}\frac{\sigma^2_n}{\sigma^2_v}} \tag{9}$$

Thus under model 5 of an independent noise affecting simultaneously u and v outputs, the relative error on the covariance estimate would be approximately 2·5 times greater than the geometrical average of the relative noise levels on each flow component (σ^2_n/σ^2_u in Equation 9 is the relative noise level, or noise to signal variance ratio, for the u component). Because of the sensitivity of uv covariances to such bi-channel noises, contaminated record segments may often be more readily detected by plotting uv covariances (or correlation coefficients) for successive record blocks, rather than individual u and v variances (Lapointe, 1990). Examples of this amplification effect will be given in the Results section.

Spectral analysis and noise detection

Equations 4 or 7 can only be used to correct variance or covariance estimates if the noise levels σ_n^2 can be estimated from the observed signals. To this end, spectral analysis can be useful to isolate and quantify narrow-band noises in turbulent flow records. Spectral analysis measures the variance contributions from different frequencies in a signal. The contribution to the overall variance of any random signal x due to fluctuations with frequencies f is expressed by the 'power density' function $P_x(f)$ and the total variance is given by:

$$\sigma_x^2 = \int_0^\infty P_x(f)\mathrm{d}f \tag{10}$$

Similarly, a pair of simultaneous signals x and y can be analysed spectrally to reveal how various frequency bands contribute to the overall covariance between the two signals. The density of covariance around a given frequency is obtained from the cospectral density function $\mathrm{COSP}_{xy}(f)$ so that:

$$\sigma_{xy}^2 = \int_0^\infty \mathrm{COSP}_{xy}(f)\mathrm{d}f \tag{11}$$

Bendat and Piersol (1986) show that if a noise component is statistically independent of the flow signal, the individual signal and noise spectra will be added together in the observed velocity spectrum (Figure 1):

$$P_{u+n}(f) = P_u(f) + P_n(f) \tag{12}$$

An important finding of research into geophysical fluid flows is that boundary-layer turbulence has some broad, universal properties. In particular, previous research (Soulsby, 1977; Panofsky and Dutton, 1984; West and Oduyemi, 1989; Kaimal and Finnigan, 1994; Lapointe, 1993) reveals that in high Reynolds number flows the turbulent velocity spectra $P(f)$ have a broad-band distribution of power with a smooth roll-off at the high frequency end, as schematized in the left-hand panel of Figure 1. Readers are referred to the geophysical literature for detailed information on typical shapes of turbulent spectra of flow signals, such as u, v or uv, in various flow conditions. When prior work has confirmed the general shape of the turbulent flow spectra in the study environment, discrete noises may be detectable as significant departures from the expected spectral shape. The noise-to-signal ratio (σ_n^2/σ_u^2) can then be evaluated by estimation of the areas under the separate u and n spectra (inverting the process in Figure 1). Pond *et al.* (1971) used this principle in atmospheric boundary-layer studies to correct u and v variance and covariance estimates corrupted by sensor platform motion. Examples of such calculations are given next.

RESULTS

Two examples of contaminated EMCM output from field and laboratory deployments are presented below

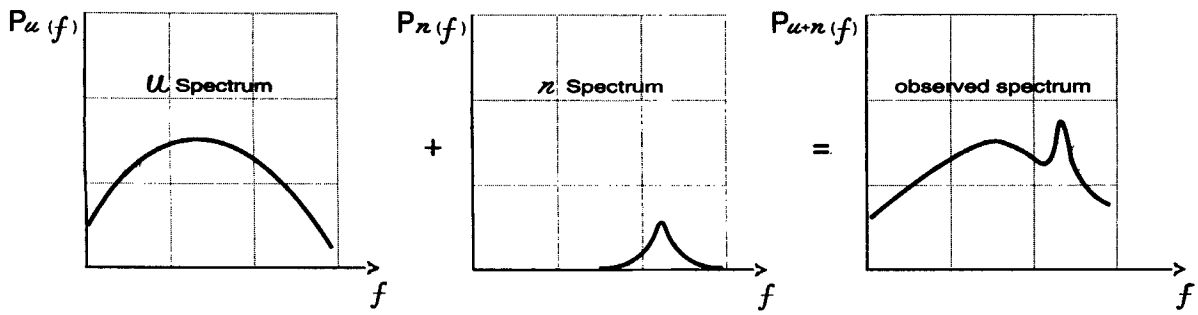

Figure 1. Schematic illustration of the additivity of flow signal (P_u) and noise (P_n) spectra when the noise signal n is uncorrelated with the flow signal u. See discussion in text. The actual shape of the turbulent flow spectrum (P_u) depends on the signal analysed (e.g. u, v, uv, etc.), the deployment conditions and the frequency response of the sensor

Table I. Deployment conditions and parameters of the spectral analysis conducted for the two examples presented in this paper. Symbols are defined in the footnote

Example	Deployment	EMCM model	Probe diameter (m)	d (m)	z (m)	U ($m\,s^{-1}$)	t_c (s)	dt (s)	f_0 (Hz)	T/T_0
1	river/ sand bed	MMB 524	0·10	2·75	0·75	0·80	0·2	0·2	0·0049	7
2	flume/ no sediment	MMB 523	0·012	0·25	0·15	0·14	0·05	0·05	0·019	6

d, flow depth; z, height of sensor above bed; U, mean flow velocity at sensor height; t_c, exponential low-pass filter time constant; dt, sampling interval; f_0, lowest frequency resolved in spectrum; T/T_0, number of successive record segments used for spectral averaging (see text)

to illustrate these principles. These examples are of course not chosen as typical of EMCM records, which have yielded invaluable data over the last decade. Their purpose is simply to illustrate how occasional noise effects, large enough to mar turbulence statistics, may best be detected by spectral analysis. Table I lists the deployment conditions for each of the examples, along with key parameters associated with the data sampling and spectral analysis. The first deployment was conducted at near-bankfull flows on the Rouge River, near St-Jovite, Canada. This meandering, sand-bedded river has a bankfull width of 100 m and a bankfull discharge of $350\,m^3\,s^{-1}$. Dunes of small amplitude (< 30 cm) covered the bed at the sampling station. More details on the deployment techniques may be found in Lapointe (1992). In example 2, turbulent flow records were collected in a 25 cm deep flow over a sediment-free bed in a non-ferrous recirculating flume measuring 10 m × 0·60 m × 0·48 m.

In both cases, Marsh McBirney (Inc.) EMCMs were used. The units measure flow in two orthogonal directions using four cocircular electrodes mounted in spherical probes of various diameters (Table I). EMCM output is generally low-pass filtered to remove high-frequency instrument noise. The sampling frequency must be chosen so that most of the variance at frequencies higher than the Nyquist frequency is removed by the low-pass filter, otherwise aliasing can degrade the spectra (Bendat and Piersol, 1986). The Marsh McBirney sensors have an inboard RC exponential low-pass filter which reduces signal variance by over one-half, for fluctuations with periods shorter than six times the time constant (Holloway, 1958). With a sampling interval equal to the RC time constant, less than 10 per cent of the variance of the true signal remains above the Nyquist frequency and aliasing is minimized (Kaimal and Finnigan, 1994).

The spectral plots are presented in the variance preserving form conventional in atmospheric and oceanic boundary layer studies (Panofsky and Dutton, 1984; Kaimal and Finnigan, 1994). In a plot of $fP(f)$ against $\log f$, relative areas under the spectrum (or cospectrum) are representative of the fraction of total variance (or covariance) between any two frequencies. To minimize the high sampling variability of spectra, replicate spectral power estimates were averaged from six or seven separate record segments of length T_0 extracted from the stationary velocity signal of total length T (Table I). This conventional technique (Bendat and Piersol, 1986; Press *et al.*, 1986) smooths out some of the sampling errors in the spectrum and better reveals the underlying broad shape of the turbulent spectrum. Assuming long enough records to reduce spectral imprecision, narrow-band noise peaks, if present, will stand out as systematic departures from the underlying turbulent spectra, as schematized in Figure 1.

Example 1: narrow-band noise in a river deployment

Figure 2A shows a 2 min series of u and v signals from the Rouge River that are representative of a longer 23·8 min record. Figure 2A displays a broad range of frequencies with no quasi-periodicity or other readily apparent signs of signal contamination. The standard deviations of the horizontal and vertical velocity relative to the mean flow velocity ($\sigma_u/U = 8$ per cent and $\sigma_v/U = 5$ per cent) are typical of boundary-layer turbulent flows in the particular deployment conditions. The location of the broad peak in the u and v spectra in

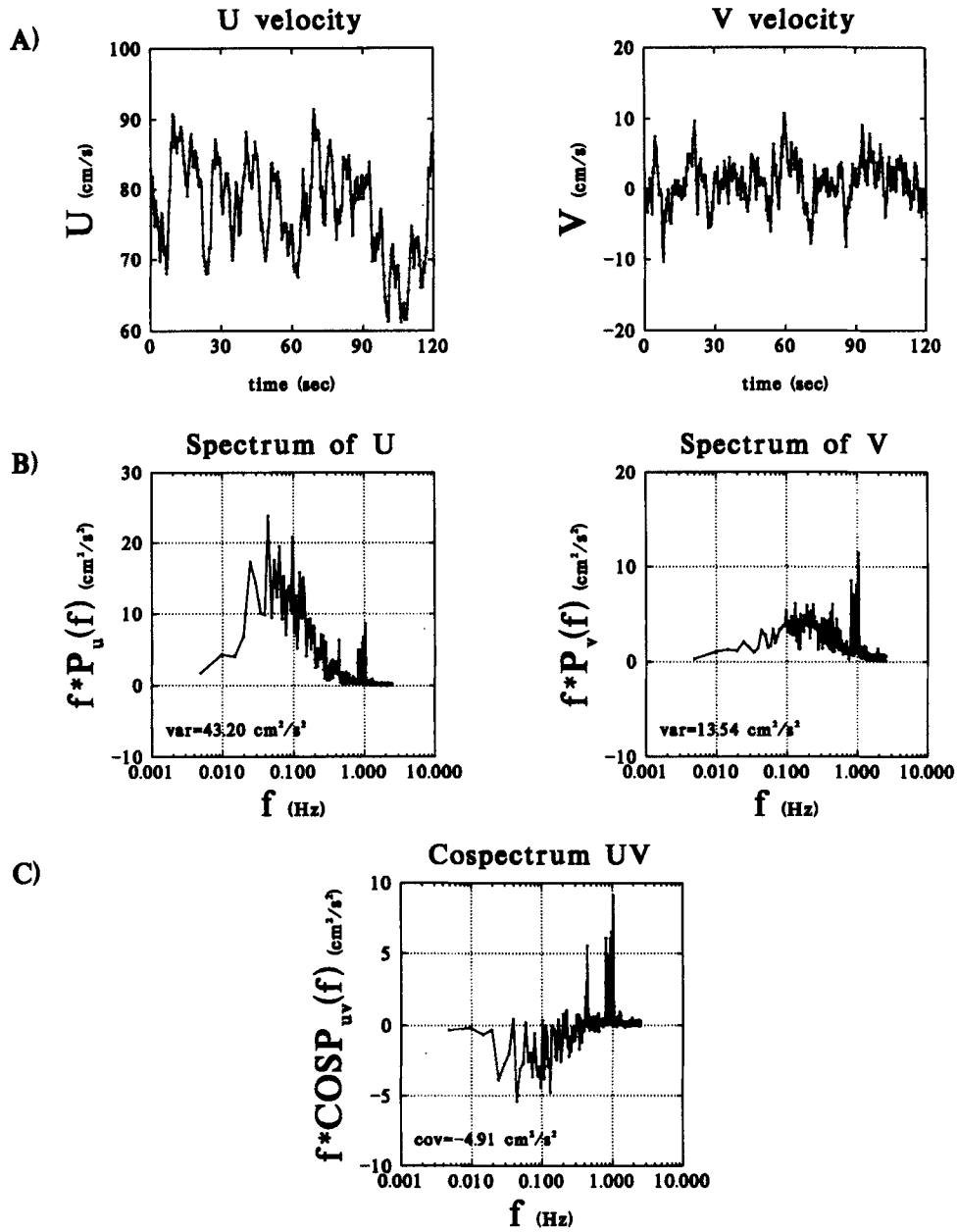

Figure 2. u, *v* spectra (B) and cospectrum (C) from an EMCM river deployment displaying narrow-band noise components around 1 Hz. These components are not conspicuous in the velocity traces (A) nor in the overall signal variances. Table I lists key parameters of the deployment conditions and signal analysis. Signal variances and covariance are shown in the panels

area-preserving form (around frequencies of 0·05 and 0·2 Hz respectively; Figure 2B) are also typical of turbulence for the given sensing distance to the wall, mean velocity U and the characteristics of the sensor used (Panofsky and Dutton, 1984; Lapointe, 1993).

However, a conspicuous, narrower second peak reaching power densities of approximately $10\,cm^2\,s^{-2}$ is also present in both spectra near 1 Hz. This noise peak is much higher than the random sampling variability of power estimates in the part of the spectrum in which it lies. These noise peaks were preserved, irrespective

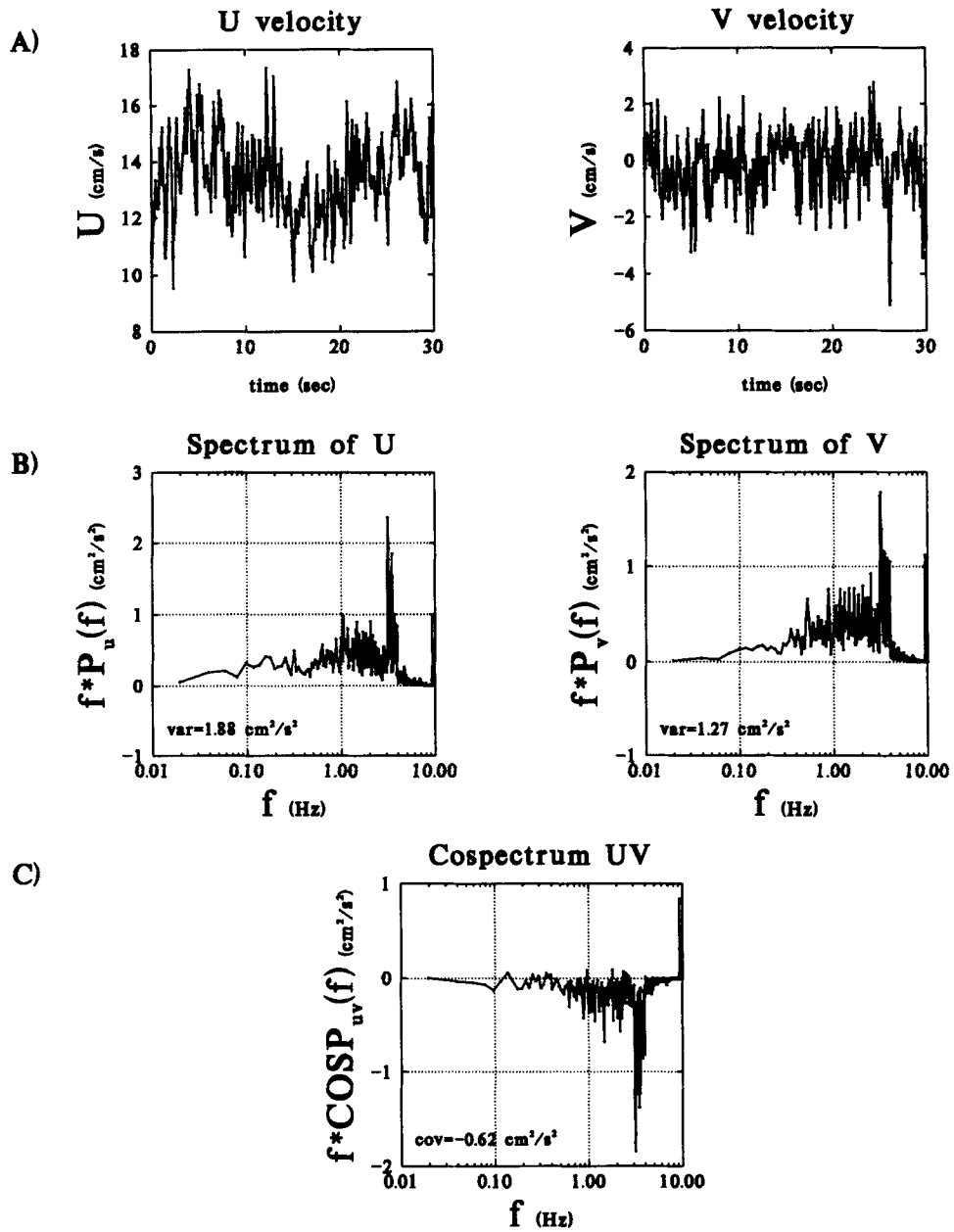

Figure 3. u, v traces (A), spectra (B) and cospectrum (C) from a flume deployment (see Table I) of an EMCM displaying narrow-band noises between 3 and 4 Hz. Signal variances and covariance are shown in the panels

of the reasonable smoothing or windowing procedures chosen for the analysis. Based on the observed areas under the noise and the interpolated flow spectra (cf. Equations 4, 12 and Figure 1), the noise-to-signal ratio on the U component (σ_n^2/σ_u^2) is only 1·5 per cent in this case, while σ_n^2/σ_v^2 is 6·5 per cent. (The relative noise level on v is greater here because the overall variance of v is smaller). Such moderate noise-to-signal ratios explain why signal contamination was not conspicuous in the traces (Figure 2A) or in the overall variance statistics.

Figure 2C presents the uv cospectrum for the same data set. The area under the cospectrum represents the

observed covariance, which was $-4{\cdot}9\,cm^2\,s^{-2}$ in this deployment. As is characteristic of boundary-layer turbulence (Soulsby, 1980; Panofsky and Dutton, 1984), the uv covariance is negative and is mostly associated with the larger eddies (represented here by frequencies under 0·2 Hz). However, discrete positive contributions to covariance can also be observed near 1 Hz and 0·4 Hz. These are linked to the noise contributions observed in both the u and v spectra. In this deployment, the noise components affecting both u and v channels were positively correlated and thus contributed positively to uv covariance as revealed by the cospectrum. In effect, the noise components here partly counteracted the negative uv covariance, typical of fluctuations in a boundary layer. Based on the areas under the observed cospectrum, the ratio of noise-induced covariance to true uv covariance $\frac{\sigma_n^2}{\sigma_{uv}^2}$ is estimated at 12 per cent. Removing the noise peak from the cospectrum would thus yield a corrected uv covariance of $-5{\cdot}6\,cm^2\,s^{-2}$.

As explained above, the relative effect on the observed covariance of the common noises on both channels was substantial (12 per cent here), even if the noise-to-signal ratio on each flow component was minor (1·5 and 6·5 per cent). This is due to the great strength of the correlation between the common noise components affecting u and v, when compared to the moderate correlation between the underlying u and v flow signals themselves (see Equations 6–8). Equation 9, based on an assumption of identical noise components (Equation 5) that are uncorrelated with the true signals u and v, predicts a covariance error of 8 per cent for this first example, while the value estimated from the cospectrum was 12 per cent.

Example 2: narrow-band noise in a flume deployment

Figure 3 presents 5 min long u and v records of turbulent flow collected by an EMCM in a laboratory flume. Smaller sensor dimensions and faster frequency response allowed higher turbulent frequencies to be monitored than in the previous example. Figure 3A shows 30 s excerpts of the u and v traces from these records, displaying the typical broad-band turbulent character. Observed signal variances were not unduly high: σ_u/U and σ_v/U values were 10 per cent and 8·6 per cent respectively, based on the 5 min record.

The u and v spectra (Figure 3B), however, show distinct noise peaks reaching power ordinates of approximately $2\,cm^2\,s^{-2}$ between 3 and 4 Hz. The noise-to-signal variance ratios, estimated as before from the spectra, are 10·2 per cent and 12·2 per cent for u and v, respectively. The common noise component again stands out clearly on the cospectrum at frequencies of 3–4 Hz (Figures 3C). Contrary to the first example, the noise components on u and v are in antiphase and so negatively correlated, here (as shown by the negative sign of the noise peak in the cospectrum). The noise thus adds to the absolute value of observed covariance in this example. The covariance contribution under the noise peak represents some 31 per cent of the remaining uv covariance. Mean downstream Reynolds stresses based on the observed signals would thus be overestimated by 31 per cent. The noise contribution to the covariance predicted from Equation 8 is 28 per cent, very close to the value of 31 per cent estimated from the observed cospectrum.

CONCLUSIONS

The paper illustrates how spectral analysis can be used to detect noises in turbulent flow records. Spectral analysis can now be conducted in minutes on PCs and should be included routinely as part of the data qualification procedures for turbulent flow records. In cases such as those illustrated here, where a narrow-band, independent noise component is clearly identifiable on the spectra, variance and covariance (shear stress) estimates can be easily corrected based on the spectral analysis.

Spectral analysis can also help to detect the presence of noise fluctuations which are substantially correlated with the flow fluctuations near the sensor. Correction procedures for such noise effects were not illustrated here as they can be far more complex and must start from the full relations (2) and (6). Finally, where noises affect a broad range of frequencies, spectral analysis may help detect the contamination but spectral separation may be more difficult to carry out.

ACKNOWLEDGEMENTS

This research was supported through NSERC funding of M. F. Lapointe and A. G. Roy.

REFERENCES

Aubrey, D. G. and Trowbridge, J. H. 1985. 'Kinematic and dynamic estimates from electromagnetic current meter data', *Journal of Geophysical Research*, **90**, 9137–9146.

Bendat, J. S. and Piersol, A. G. 1986. *Random Data: Analysis and Measurement Procedures*, 2nd edn, Wiley, New York, 566.

Clifford, N. J., French, J. R. and Hardisty, J. (Eds). 1993. *Turbulence: Perspectives on Flow and Sediment Transport*, Wiley, Chichester, UK, 360.

Guza, R. T., Clifton, M. C. and Rezvani, F. 1988. 'Field intercomparisons of electromagnetic current meters', *Journal of Geophysical Research*, **93**, 9302–9314.

Heathershaw, A. D. 1979. 'The turbulent structure of the bottom boundary layer in a tidal current', *Geophysical Journal of the Royal Astronomical Society*, **58**, 395–430.

Holloway, J. L. 1958. 'Smoothing and filtering of time series and space fields', *Advances in Geophysics*, **4**, 352–388.

Kaimal, J. C. and Finnigan, J. J. 1994. *Atmospheric Boundary Layer Flows; their Structure and Measurement*, Oxford University Press, New York, 289.

Lane, S. N., Richards, K. S. and Warburton, J. 1993.'Comparison between high frequency velocity records obtained with spherical and discoidal electromagnetic current meters', in Clifford, N. J., French, J. R. and Hardisty, J. (Eds), *Turbulence: Perspectives on Flow and Sediment Transport*, Wiley, Chichester, UK, 121–164.

Lapointe, M. F. 1990. *Intermittent Turbulent Suspension Events over Sand Dunes on the Bed of the Fraser River, near Mission, British Columbia*, Ph.D. dissertation, University of British Columbia, 142.

Lapointe, M. F. 1992. 'Burst-like sediment suspension events in a sand bed river', *Earth Surface Processes and Landforms*, **17**, 253–270.

Lapointe, M. F. 1993. 'Monitoring alluvial sand suspension by eddy correlation', *Earth Surface Processes and Landforms*, **18**, 157–175.

McQuivey, R. S. 1973a. *Principles and Measuring Techniques of Turbulence Characteristics in Open-Channel Flows*, USGS Professional Paper, **802-A**.

McQuivey, R. S. 1973b. *Summary of Turbulence Data from Rivers, Conveyance Channels and Laboratory Flumes*, USGS Professional Paper, **802-B**.

Panofsky, H. A. and Dutton, J. A. 1984. *Atmospheric Turbulence: Models and Methods for Engineering Applications*, Wiley, New York, 390.

Pond, S., Phelps, G. T., Paquin, J. E., McBean, G. and Stewart, R. W. 1971.'Measurement of the turbulent fluxes of momentum, moisture and sensible heat over the ocean', *Journal of Atmospheric Science*, **28**(6), 901–917.

Press, W. H., Flannery, B. P., Teukolsky, S. A. and Vetterling, W. T. 1986. *Numerical Recipes: the Art of Scientific Computing*, Cambridge University Press. Cambridge. 118.

Soulsby, R. L. 1977. 'Similarity scaling of turbulence spectra in marine and atmospheric boundary layer', *Journal of Physical Oceanography*, **7**, 934–937.

Soulsby, R. L. 1980. 'Selecting record length and digitization rate for near-bed turbulence measurements', *Journal of Physical Oceanography*, **10**, 208–219.

West, J. R. and Oduyemi, K. O. K. 1989. 'Turbulence measurements of suspended solids concentration in estuaries', *Journal of the Hydraulics Division*, ASCE, **115**, 457–474.

Williams, J. J., Thorne, P. D. and Heathershaw, A. D. 1989. 'Measurement of turbulence in the benthic boundary layer over a gravel bed', *Sedimentology*, **36**, 959–971.

Willmarth, W. W. and Lu, S. S. 1972. 'Structure of the Reynolds stress near the wall', *Journal of Fluid Mechanics*, **55**, 65–92.